American Mineralogist, Volume 82, pages 1091–1100, 1997

Epitaxial overgrowth of goethite on hematite synthesized in phosphate media: A scanning force and transmission electron microscopy study

VIDAL BARRÓN,[1] NATIVIDAD GÁLVEZ,[1] MICHAEL F. HOCHELLA JR.,[2] AND JOSÉ TORRENT[1]

[1]Departamento de Ciencias y Recursos Agrícolas y Forestales, Universidad de Córdoba, Apdo. 3048, 14080 Córdoba, Spain
[2]Department of Geological Sciences, Virginia Polytechnic Institute and State University, Blacksburg, Virginia 24061, U.S.A.

ABSTRACT

We used X-ray diffraction (XRD), scanning force microscopy (SFM), transmission electron microscopy (TEM), and color to investigate the effect of phosphate on the crystallization rate, nature, and morphology of iron oxides prepared from ferrihydrite in the laboratory. Synthesis was performed at two temperatures (323 and 373 K) and two pH values (9 and 12) from ferric nitrate, for P/Fe atomic ratios ranging from 0 to 2.5%. The presence of phosphate retarded crystallization, tended to favor hematite over goethite, and markedly influenced the morphology of the goethite crystals formed at high pH. Application of SFM in the deflection mode was useful to investigate the morphology of the small goethite crystals, with careful attention paid to operating conditions; in particular, sharp silicon probes were found to produce fewer artifacts than coarser silicon nitride ones. At low P/Fe ratios (<0.2%), the goethite crystals were thin, elongated, multidomain laths; at high P/Fe ratios (>1.5%), star-shaped, twinned crystals were produced. All the theoretical shapes, derived from the assumption that star-shaped crystals result from the epitaxial growth of goethite on a hematite core, were observed by SFM and TEM. The presence of such hematite nuclei was supported by XRD, selected-area electron diffraction, color, and preferential dissolution of the samples in HCl, because it is known that hematite dissolves faster than goethite in acid. With increasing P/Fe ratio, the arms of the star-shaped crystals became shorter. This was likely due to the higher density of P-adsorbing pairs of singly coodinated OH groups on terminal {021} faces relative to prismatic {110} arm faces.

INTRODUCTION

The laboratory synthesis of various iron oxides (a term used here to indicate iron oxides, hydroxides, and oxyhydroxides) has provided a better understanding of the origin and behavior of these oxides in natural environments, as well as the basis of their industrial applications (e.g., Schwertmann and Taylor 1989; Schwertmann and Cornell 1991; and references therein). Synthesis variables that have been explored include, among others, temperature, pressure, starting materials, formation additives, and pH. They modify the crystallochemical nature of the ferric (hydr)oxide grown and affect properties such as adsorption behavior, aggregation, and color.

Regarding formation additives, iron oxides have been synthesized in the presence of trace to minor amounts of Al and Si, transition metals (Ti, Mn, Co, Cu, and Zn), organic acids (citric, tartaric, oxalic, and lactic), and phosphate (a review of synthesis additives is given in Cornell et al. 1989, or more recently in Cornell and Schwertmann 1996). The present study concerns phosphate because of its importance in soil fertility, and its association with and presumed inhibitory effects at relatively low solution concentrations on the formation of hematite and goethite. Occasionally, fertilizer phosphate can be a major cause of freshwater eutrophication. Therefore, it is important to investigate the fate of excess phosphate in soil, particularly the amount that can be adsorbed onto or occluded within iron oxides during their nucleation and growth, and how it can influence the crystallization of such oxides.

Several studies have described the influence of phosphate on the formation of ferric and ferrous iron oxides (Barton 1990; Schwertmann 1969; Reeves and Mann 1991; Kandori et al. 1992; Morales et al. 1992; Matijevic 1993; Sugimoto et al. 1993; Ocaña et al. 1995). These papers, except Kandori et al. (1992), deal with the mechanism of formation of ellipsoidal hematite particles from ferric salt solutions in the presence of small amounts of phosphate. Nevertheless, no mention has ever been made of morphology modification of goethite in the presence of phosphate. Morphology, however, plays a key role in controlling the surface area per unit mass of the oxide, as well as the crystal faces (and their specific reactivity) that dominate that surface area. Furthermore, the iron oxide-phosphate system has never been studied with scanning force microscopy (SFM). Scanning probe microscopy (SPM; this includes both scanning tunneling microscopy and SFM) should be apt for this type of study. SPM can image details on surfaces down to the sub-nanometer range, and it can also be used to measure

0003–004X/97/1112–1091$05.00

angles between faces for easier crystallographic identification. Furthermore, it can be performed under ambient conditions, and it is often easier to use than electron microscopy.

SPM has already been the basis of several studies involving the characterization and chemical reactivity of iron oxides (Eggleston and Hochella 1992; Eggleston and Stumm 1993; Maurice et al. 1995; Junta-Rosso and Hochella 1996; Weidler et al. 1996; Fischer et al. 1996). To our knowledge, except for Weidler et al. (1996) and Fischer et al. (1996), all this work was performed using natural large single-crystal fragments of specular hematite. Weidler et al. (1996) used SFM to observe the existence of vicinal faces on the {100} plane of minute crystals of synthetic goethite. Fischer et al. (1996) described the surface microtopography of a synthetic submicrometer goethite grain.

In this study we use SFM to examine the influence of phosphate on the morphology of minute hematite and goethite crystals synthesized from Fe^{3+} solutions at alkaline pH and at two different temperatures (323 and 373 K). The SPM literature on very small mineral particles is scarce. Besides Weidler et al. (1996) and Fischer et al. (1996), only Lindgreen et al. (1991), Blum (1994), and Nagy (1994) have studied ultrafine mineral particles with SFM, and these latter studies dealt with silicate clays. The platy morphology of silicate clays allows a relatively straightforward interpretation of their SFM images. However, this is not the case for nano-sized ultrafine particles of different shapes. In this study, we also briefly explore the interpretation of SFM images of minute particles and compare this with the information gained from transmission electron microscopy (TEM) images of the same particles. This comparison indicates that SFM will become indispensable for imaging small particles, because it adds valuable information not easily available from TEM imaging. Unfortunately, SFM is also subject to artifacts that can easily be misinterpreted.

Materials and methods

Preparation of the iron oxides

Two series of iron oxides were crystallized by storing aqueous suspensions of freshly precipitated ferrihydrite at 323 and 373 K for 2 months and 2 weeks, respectively, in capped polypropylene bottles placed in low-temperature ovens. Ferrihydrite suspensions were obtained by mixing Fe, as nitrate, plus P as phosphate, in different atomic ratios (P/Fe: 0, 0.16, 0.5, 1.5, and 2.5%) and titrating the mixtures to pH 9 or 12. The first stages of crystallization occured with the development of small polynuclear species of iron hydroxides (Cornell et al. 1989). This is accompanied by a relatively fast initial decrease in pH, followed by slower changes with time. Therefore, the pH was periodically readjusted back to the target value as needed during the storage periods. We attempted to prevent the pH from drifting more than 1 pH unit, and this only for relatively short times (<5 h). Buffers were not used, which simplified the solution chemistry and surface interaction possibilities.

The crystallized products were washed of residual salts by successive decanting after centrifugation in deionized distilled water. Finally, the suspensions were placed in dialysis membranes immersed in deionized water until the electrical conductivity of the equilibrium water was below 10^{-3} S/m.

Chemical and mineralogical analysis

The amount of residual ferrihydrite in the products of the experiments described above was measured by acid oxalate extraction (Schwertmann 1964). The proportions of goethite and hematite in the products were estimated from X-ray powder diffraction (XRD) with a Siemens D5000 instrument using monochromatized CoKα radiation. Mixtures of goethite and hematite of crystal sizes similar to those of the products synthesized were used as external standards. Calibration curves were obtained for the range in the hematite/(hematite + goethite) ratio of 0.01–0.99. The mixtures were step-scanned for 10 s at 0.01° 2θ steps, and the peak area of the hematite 012, 110, and goethite 110, 130, and 111 peaks were used for the calibration. This procedure provides good semiquantitative estimates of both minerals and detection limits of less than 1% for mixtures containing only hematite and goethite. The color of the powder samples was measured spectrophotometrically as described by Barrón and Torrent (1986).

TEM was performed with a JEOL JEM-200 CX microscope operating at 120 kV. Samples were prepared for microscopic analysis by dispersing a minute portion of sample in acetone and placing a drop on a carbon-coated copper grid. SFM was performed using a Digital Instruments Nanoscope III; all images in this paper are in deflection mode. A brief explanation of this mode of imaging is given here. During SFM imaging, an error signal is continuously computed. This error signal is the deviation of the probe deflection from where the operator set it to be maintained by adjusting the setpoint voltage on the microscope. It is solely this error signal that is used to generate the deflection image, along with the *X*-*Y* position of the probe. Therefore, the deflection mode image is effectively slope-encoded like height mode SFM, SEM, or optical images. The advantage of deflection mode images is that they are excellent for emphasizing fine detail in surface microtopography (easily down to the nanometer scale), clearly showing subtle features that may not be as apparent in height mode SFM. Their disadvantage is that the images contain no height information. Therefore, the cross-section shown in this paper was obtained from a height image that was collected simultaneously with the deflection image.

The heart of the SFM technique is the tip, or probe, used for imaging. Two kinds of SFM probes were used in this study: (1) conventional silicon nitride (Si_3N_4) probes (purchased through Digital Instruments) with pyramidal shape, a solid angle between 70° and 90° (de-

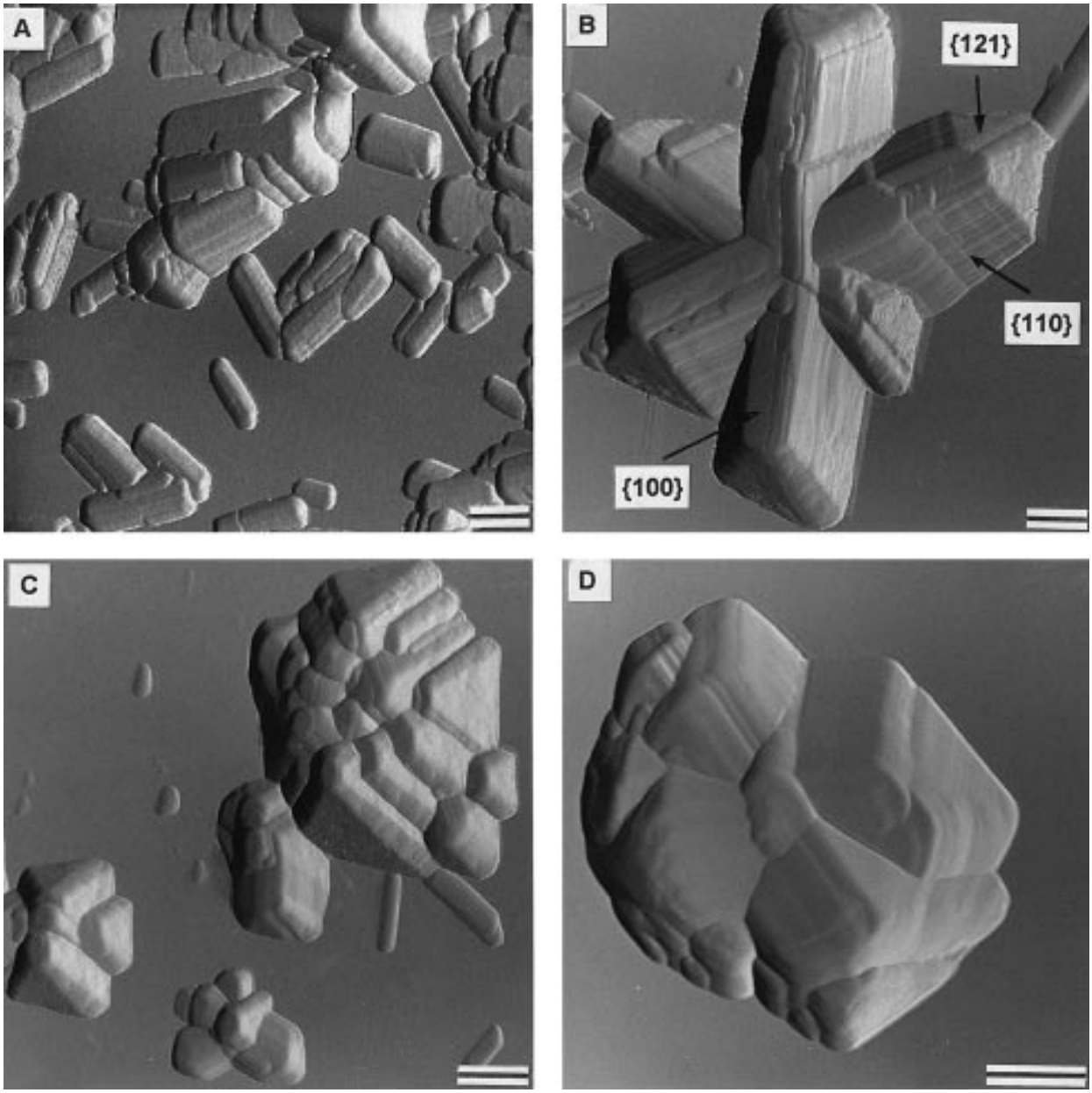

FIGURE 1. SFM images obtained with conventional silicon nitride probes of different samples synthesized at 373 K, pH 12, and a P/Fe atomic ratio of (**A**) 0%, (**B**) 1.5%, and (**C** and **D**) 2.5%. Bars represent 200 nm. The {121} and {100} faces shown in (**B**) are artifacts produced by the conventional probe.

pending on orientation of the probe relative to the direction of scan), and an end radius of curvature of about 50 nm, and (2) etched-silicon probes (manufactured by Nanosensors, purchased through Digital Instruments) with a solid angle between 20° and 50°, but decreasing to a maximum of approximately 20° within 200 nm of the end of the probe, and an end radius of curvature between 5 and 10 nm. The silicon nitride probes are far less expensive and more durable, but image artifacts because of probe shape can be much more severe with them, especially when imaging minute particles, as is the case with this study (these artifacts are discussed below). Except for Figure 1, which is included to show dramatic image artifacts obtained by using the silicon nitride probes, all images presented and discussed in this paper were collected with the etched silicon probes.

We mounted the iron oxide particles on muscovite surfaces for SFM imaging because muscovite is atomically smooth over large regions. Nevertheless, the etched silicon probes (because of their shape) tended to push the minute iron oxide particles around during scans in air, no matter how careful we were in minimizing the tracking

TABLE 1. Iron forms synthesized at different temperatures, pH values, and P/Fe atomic ratios

	373 K				323 K			
	pH 12		pH 9		pH 12		pH 9	
P/Fe*	Fe_o/Fe_t†	R‡	Fe_o/Fe_t†	R‡	Fe_o/Fe_t†	R‡	Fe_o/Fe_t†	R‡
0.00	1.4	0	1.9	80	0.7	0	0.8	82
0.16	1.3	0	1.4	82	0.5	0	0.7	86
0.50	1.3	0	1.5	98	0.5	1	0.9	99
1.50	1.1	1	1.1	2	0.7	10	2.8	2
2.50	0.9	2	41.7	§	0.7	7	83.0	§

* Atomic ratio × 100.
† (Oxalate-extractable Fe/total Fe) × 100.
‡ [Hematite/(hematite + goethite)] × 100.
§ No quantitative estimation of hematite and goethite was made when Fe_o/Fe_t was high.

force. Through trial and error, we found that well-dispersed particles in solution (obtained by sonication) could be attached to the muscovite surface by quickly adjusting the pH to 4, placing a drop on the substrate, and allowing it to evaporate quickly.

To better understand possible epitaxial relationships between the atomic structures of hematite and goethite, atomic models for different crystallographic planes of both minerals were computed using the program XTALDRAW (Gibbs et al. 1996). Atomic positions from the refined structures of hematite and goethite after Blake et al. (1966) and Forsyth et al. (1968), respectively, were used as inputs to XTALDRAW.

RESULTS AND DISCUSSION

Reaction products

A summary of the conditions of each growth experiment and their products is given in Table 1. The effect of phosphate as an inhibitor to the crystallization of hematite and goethite from ferrihydrite was only apparent at pH 9 and a P/Fe atomic ratio of 2.5%, which we found had the highest Fe_o/Fe_t ratios. Nevertheless, a slower rate of crystallization was observed in the presence of phosphate in agreement with previous work (Cornell et al. 1987; Cornell et al. 1989). More recently, Kandori et al. (1992) found that products prepared at pH 12, a P/Fe atomic ratio of 1%, in 4 days at 303 K were poorly crystalline, and contained very fine particles of goethite (with a high specific surface area and microporosity). We suspected that this result might be rate dependent. It is evident from our study that an extended period and a higher temperature of aging (two months for the experiments at 323 K) can overcome the retardation effect of phosphate, as our products at pH 12 and a P/Fe ratio of 1.5 or 2.5% indicated.

Because the sorption of phosphate on ferrihydrite is influenced electrostatically (Bowden et al. 1980), a high pH should disfavor phosphate adsorption and, consequently, its inhibitory effect on crystallization. In fact, the amounts of phosphate retained in our products, in relation to the initial P/Fe proportion in the synthesis reagents, were much smaller in samples prepared at low pH than at high pH (N. Gálvez et al., in preparation).

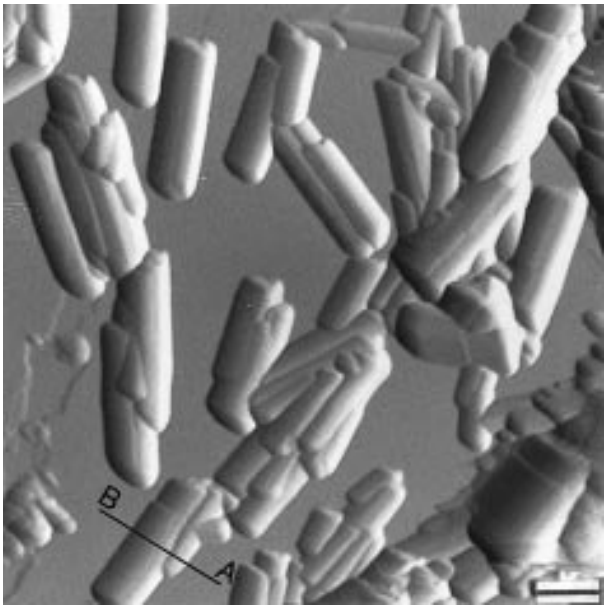

FIGURE 2. SFM image using a sharp Si tip of goethite synthesized at 373 K, pH 12, and in the absence of phosphate. Bar represents 200 nm. The particle cross-sectioned in Figure 6 is marked in the bottom left corner.

It has also been established (Schwertmann 1969) that phosphate favors hematite over goethite formation. This is certainly the case in our experiments at pH 9 for P/Fe atomic ratios of 0.16 and 0.5%; however, for higher P/Fe atomic ratios, either goethite is the dominant crystalline product or only ferrihydrite and goethite are present.

At pH 12 the products are well crystallized (Fe_o/Fe_t is below 1.5% in all cases) and, according to the XRD data, goethite is either the dominant or the only crystalline product. Minor amounts of hematite are formed at atomic P/Fe ratios over 0.5%. Quantification of these amounts was difficult, because the highest intensity peak for hematite, 104, coincides with a major line of goethite, 130, and only the very small 012 and 110 hematite peaks were used to quantify this mineral. The increasing proportion of hematite with increasing P/Fe atomic ratio is corroborated by the color of the products. So, for the products prepared at 373 K, and according to the Munsell notation (Munsell Color Company 1975), the color changes from 0.2Y 5.6/6.0 (brownish yellow) for the sample without P, to 9.1YR 7.1/7.1 (reddish-brownish yellow) and 5.4 YR 5.9/7.8 (reddish yellow) for the samples with P/Fe atomic ratio of 1.5 and 2.5%, respectively. We discuss below the presence of hematite in these products using SFM and TEM images and selected-area electron diffraction patterns.

Comparison of pyramidal and sharp probes

The deflection mode SFM images obtained with conventional silicon nitride probes (Figures 1A–D) show

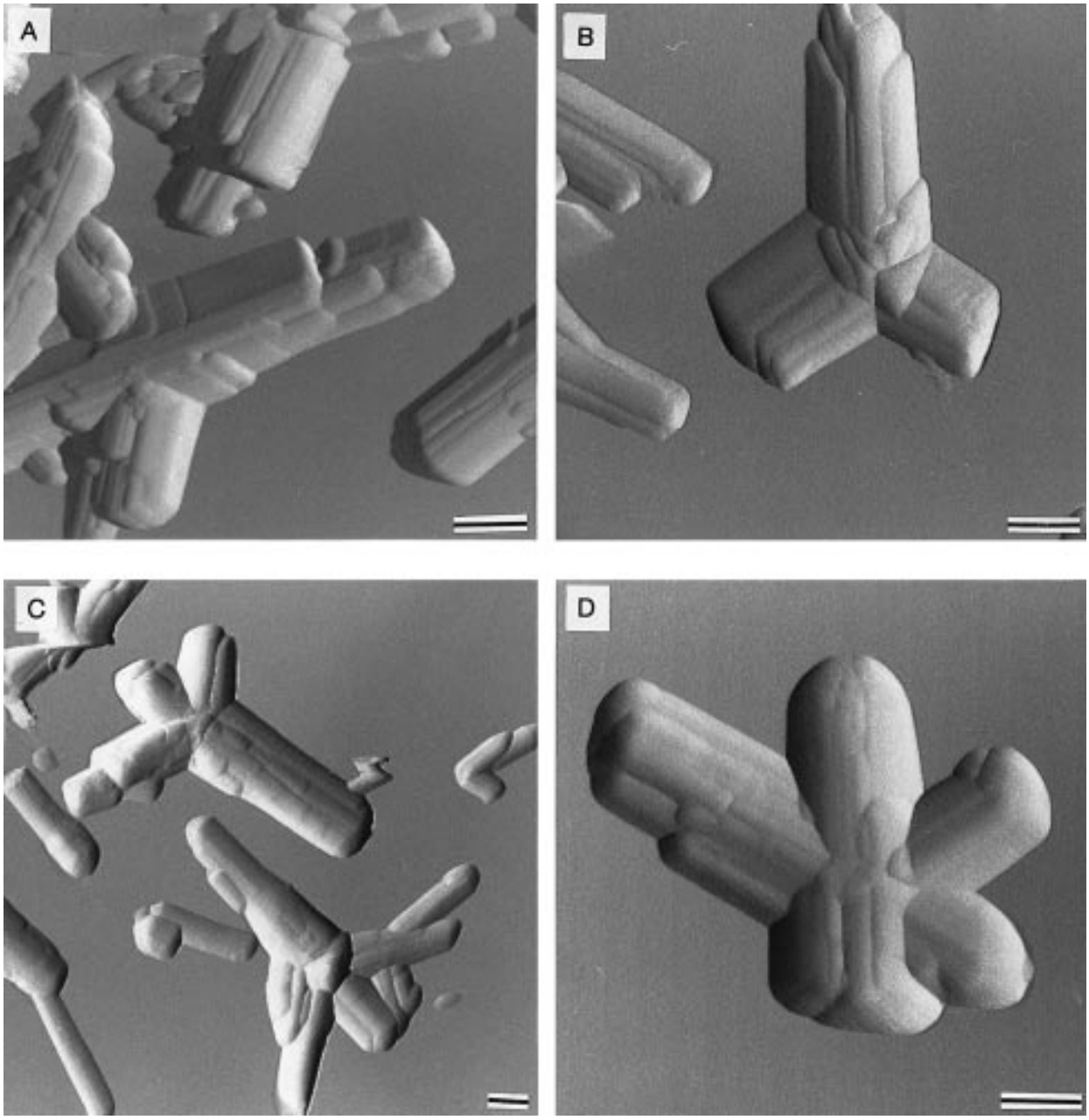

FIGURE 3. SFM images using a sharp Si tip of a sample synthesized at 373 K, pH 12, and in the presence of a P/Fe atomic ratio of 1.5% showing different star formations. Bars represent 200 nm.

prismatic and radiating crystals seemingly terminated by distinctive, higher index faces. After measuring interfacial angles by means of cross-sectional analysis of SFM images, one can apparently identify typical goethite faces, for example, {100} as prismatic faces and {121} as terminating faces. Weidler et al. (1996), by using the same type of silicon nitride probes, also found that goethite needles were bounded by the same faces; they also showed parallel rills running along the {110} faces. In fact, our images in Figure 1 look remarkably similar to theirs.

When we imaged the same samples with the much sharper etched-silicon probes, we never observed the higher index terminating faces or the rills running along the {110} faces (Figs. 2–4). Furthermore, the TEM micrographs (Fig. 5) seem to indicate that the terminations are rather more vertical than the ones that correspond to {121} faces. In addition, from a TEM image of a thin section of an acicular goethite cut perpendicular to the crystallographic *c* direction, Schwertmann (1984) showed that the apparent {100} face is really formed by {110} faces.

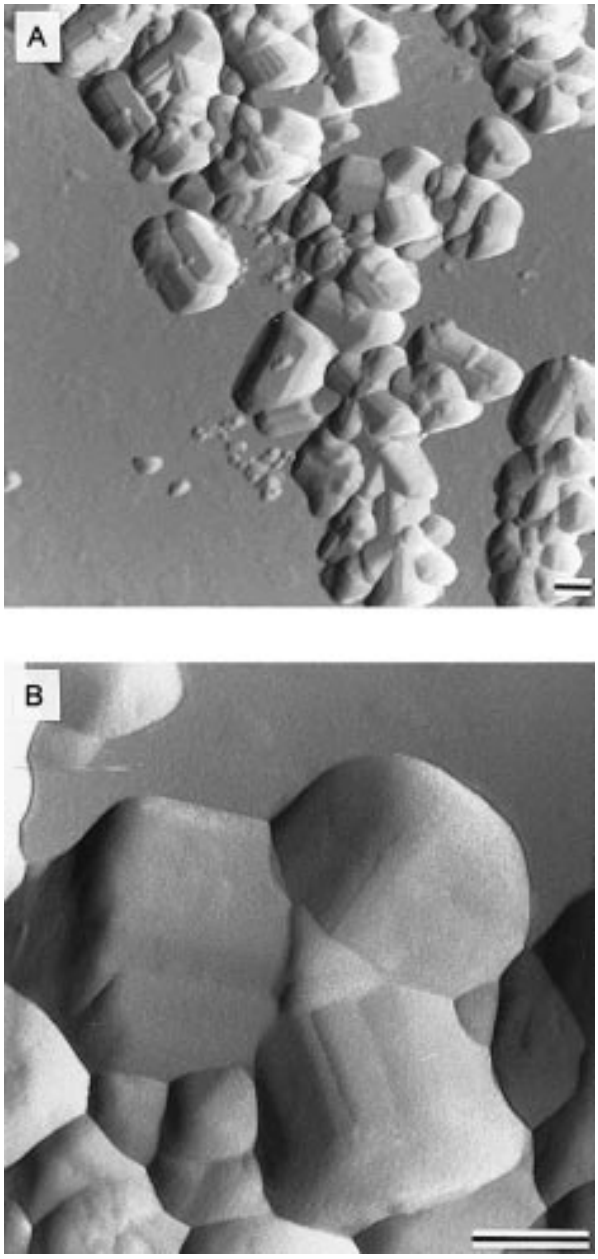

FIGURE 4. SFM images using a sharp Si tip of a sample synthesized at 373 K, pH 12, and in the presence of a P/Fe atomic ratio of 2.5%. (**B**) is a magnified image of a selected zone from (**A**). Bars represent 200 nm.

It has also been shown, for example in ''spines'' of naturally occurring MnO_2 and various clay minerals (Eggleston 1994; Blum 1994), that if surface topography has angles more vertical than the solid half angle of the probe (approximately 45–55° from the horizontal in the case of silicon nitride probes), one necessarily obtains imaging probe artifacts. For surfaces that have both these angles and high relief, these artifacts can be dramatic and dominate the images. Even the very sharp etched-silicon probes show imaging artifacts, but they are much less pronounced. For example, after analyzing one of our cross sections (Fig. 6), we could assign {120} faces to some of our goethite crystals according to their apparent angles with {110} faces. However, for this to occur {120} faces should terminate at the surface of the mica. This would only be possible if the crystal would lie on a perfect, large {100} face, another unlikely face for goethite. Thus it is important to keep in mind the limits imposed by different probes before interpreting SFM images. Hereafter, only SFM images collected with the etched-silicon probes are discussed.

Effect of P on the crystal morphology and epitaxial growth of iron oxides

Very few morphological differences were observed between samples prepared at different temperatures. When only small amounts of phosphate (P/Fe = 0.16%) or no phosphate was present, most goethite crystals were lath shaped and elongated along the *c* crystallographic direction. From the SFM images (Fig. 2), one can observe distinctive multi-domain crystals that have their surface area dominated by {110} faces. SFM cross-sections (Fig. 6) show that the different domains are joined by {110} faces along the *c* axis as previously observed by Schwertmann (1984). Cornell and Giovanoli (1986), from cross-section micrographs, also reported that these intergrowths appear to have a small region of nucleation in the center and then grow in the [001] direction. However, there is a possibility that this observation could be due to a distortion caused by pressure when these particles are sectioned with a diamond knife. From our SFM images, steps running in a direction along the {110} faces could be intergrowths, consistent with a previous high-resolution electron microscopy study by Cornell et al. (1983). This study showed that the twins were highly coherent across the domain boundaries.

The effect of phosphate on crystal morphology in our experiments becomes apparent with a P/Fe atomic ratio of 0.5% (Figs. 3, 4, and 5B–D). At this point, we observed different kinds of star-shaped crystals and also some very narrow and long single crystals associated with the stars.

Naturally occurring twinned crystals of goethite with the characteristic star shape encountered here were described long ago by Lapparent (cited by Atkinson et al. 1968). This shape has been previously explained as resulting from the epitaxial growth of goethite starting from a nucleus of hematite (Atkinson et al. 1968), whose formation is favored at pH $<$ 12. From a crystallographic point of view, the atomic configuration of O atoms on the hematite {100} and the goethite {001} match reasonably well, providing for epitaxial growth (we have portrayed this in Fig. 7 by drawing the hematite and goethite structures projected on the two planes perpendicular to the epitaxial surfaces). One can also expect an overgrowth of goethite from six equivalent {100} hematite planes, consistent with the hexagonal structure of this

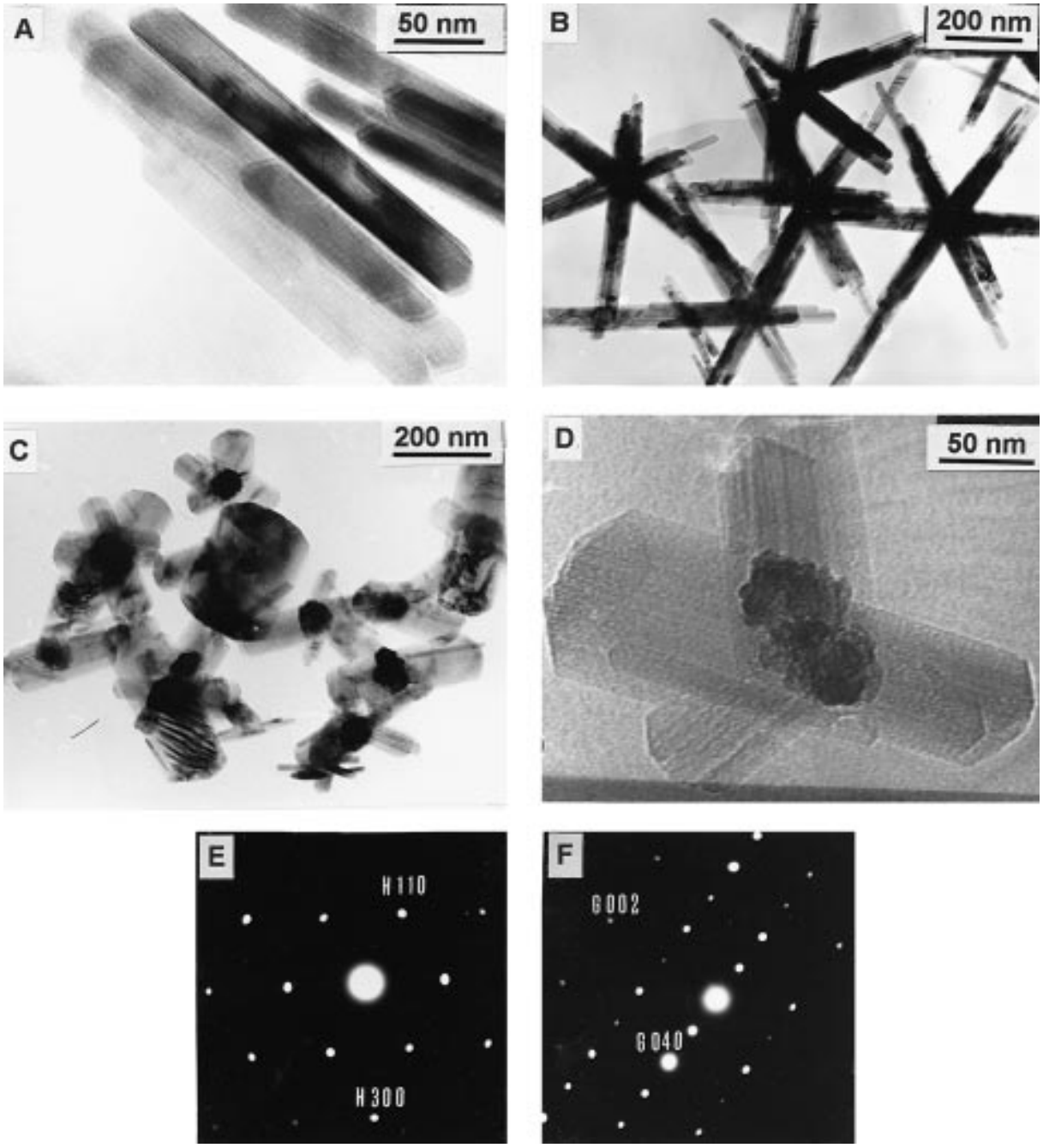

FIGURE 5. Electron micrographs of samples synthesized at 373 K, pH 12, and in the presence of a P/Fe atomic ratio of: (**A**) 0%, (**B**) 1.5%, and (**C** and **D**) 2.5%. (**E**) and (**F**) are the electron diffraction patterns of the core and arm areas shown in (**D**).

mineral. Accordingly, we imaged with SFM (Figs. 2–4) and TEM (Figs. 5B–D) star formations consisting of 2–6 arms.

The TEM images of the sample obtained at 373 K and P/Fe atomic ratio of 2.5% (Figs. 5C–D) show star-shaped crystals that have a core with a higher electron density than that of the arms. This core yields the electron diffraction pattern of hematite, whereas the arms yield that of goethite (Figs. 5E–F). Hematite was identified in this sample by XRD, but the semiquantitative estimate for it was only 2%, i.e., a proportion smaller than that suggested by the TEM images. This might be due to the fact that, in randomly oriented powder samples, the star core is hidden from the X-ray beam in many of the possible star orientations. The hematitic nature of the core is further substantiated by: (1) the redder color of this sample relative to pure goethite samples prepared at smaller P/Fe ratios, as discussed before, and (2) the preferential core

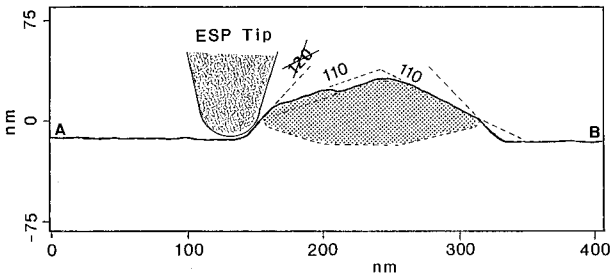

FIGURE 6. Cross section from an SFM image of a goethite particle showing a parallel growth on {110} faces and a false {120} face as consequence of a tip artifact.

dissolution that was observed when the samples imaged in Figure 4 were treated with 6 M HCl for 2 h (Fig. 8A). The observation that hematite dissolves faster than goethite in HCl is well documented in the literature (Cornell et al. 1974; Sidhu et al. 1981; Schwertmann 1987), and Cornell et al. (1974) showed TEM images of blocky particles of synthetic iron oxides with the center partly dissolved by acid. Further support to the idea that the star core is hematite is that, upon HCl etching, the color of the sample changed from 5.4 YR 5.9/7.8 (reddish yellow) to 8.9YR 6.2/6.5 (brownish-reddish yellow). On the other hand, TEM images gave no evidence of crystals in the sample other than the typical goethite stars.

The TEM images of the sample synthesized at 373 K and a P/Fe ratio of 1.5% (Fig. 5B) show star centers not distinctly darker than the arms. However, this sample contains 1% hematite, as estimated by XRD, is significantly redder than the samples prepared without P, and shows dissolution features at the center of the stars after treatment with HCl (Fig. 8B). As in the sample considered earlier, color becomes yellower upon HCl etching. Therefore, in analogy with the former sample, one can assume the presence of at least minute hematite cores in some particles.

For the samples prepared at pH 12, 323 K, and high P/Fe ratios, star-shaped goethite crystals were also seen in the TEM images (not shown). The 373 and 323 K series differed in that, in the latter, hematite was identified by XRD in the 0.5% P/Fe ratio sample, and the proportion of hematite in the high-P samples was larger. It is possible that the longer crystallization time of the 323 K series may have promoted better growth of hematite crystals.

In the series prepared at pH 9, hematite is dominant, both at 373 and 323 K, for P/Fe ratios up to 0.5%. This is expected because, at slightly to moderately alkaline pH values, hematite is favored over goethite (Cornell and Schwertmann 1996). In these samples, part of the goethite grows epitaxially over the more abundant hematite crystals (Fig. 9), as found by others (Schwertmann 1965; Cornell and Giovanoli 1985).

The former results support the contention that star-shaped goethite crystals result from epitaxial growth of goethite on hematite. In our series, such twinned crystals

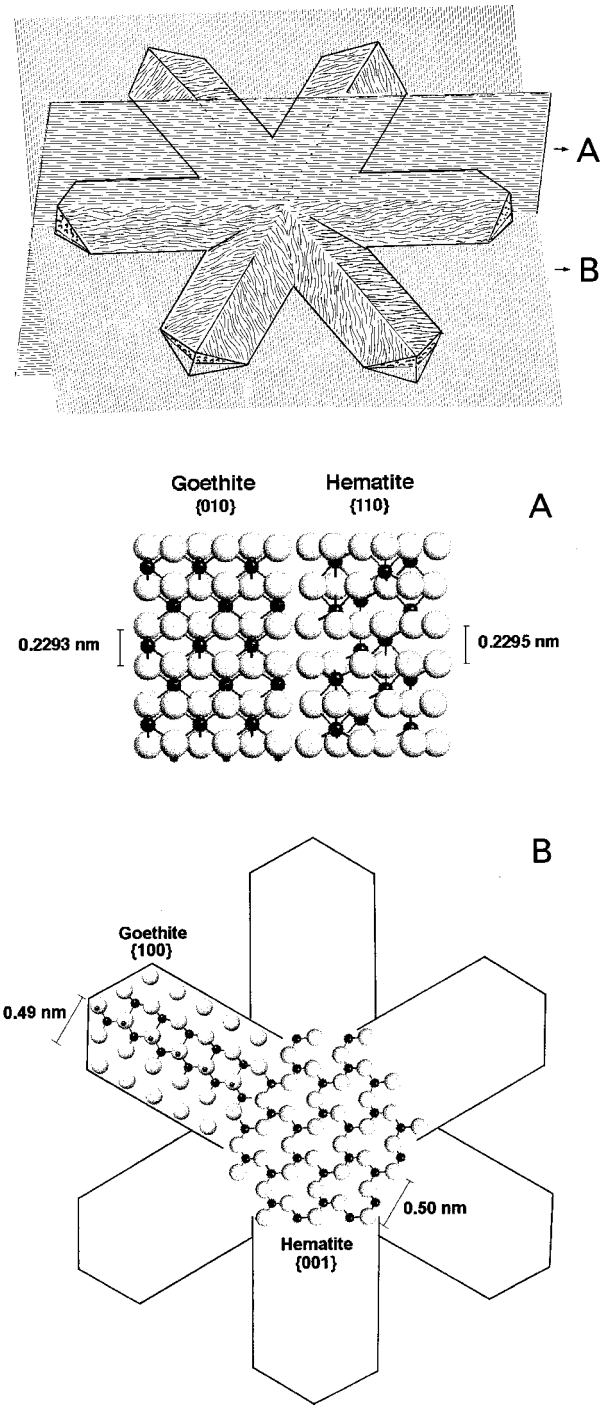

FIGURE 7. Atomic configuration of O atoms for the epitaxial overgrowth of goethite on hematite for the two planes sketched in the upper figure.

were observed only in samples with evidence of hematite cores, either directly (electron diffraction, XRD) or indirectly (color, dissolution features). There seems to be a continuum between epitaxial growth of small goethite arms on large hematite crystals and almost pure goethite-

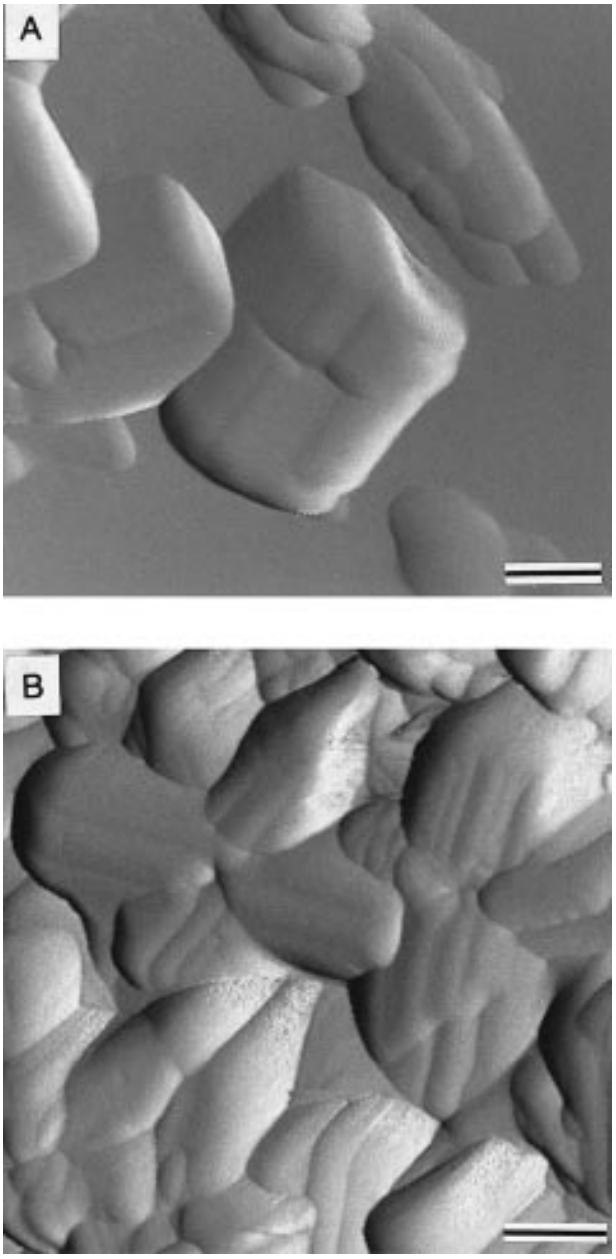

FIGURE 8. SFM images using a sharp Si tip of samples synthesized at 373 K, pH 12, and in the presence of a P/Fe atomic ratio of (**A**) 2.5% and (**B**) 1.5%, after treatment with 6 M HCl for 2 h. Bars represent 200 nm.

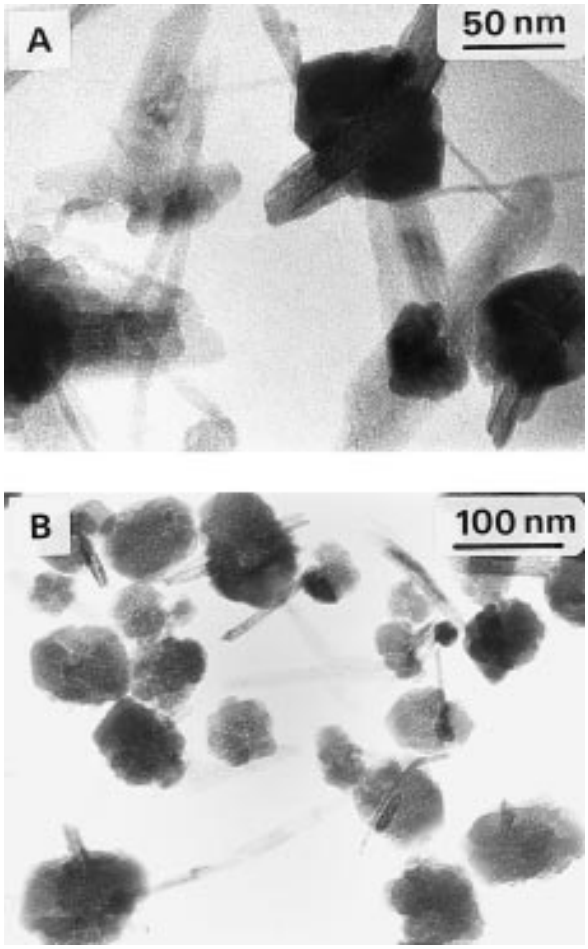

FIGURE 9. Electron micrographs of samples synthesized at 323 K, pH 9, and in the presence of a P/Fe atomic ratio of (**A**) 0% and (**B**) 0.16%.

twinned crystals. At this point, the question of whether the formation of goethite-twinned crystals requires a hematite core, however small this may be, remains unresolved.

At the higher phosphate concentrations (P/Fe = 2.5%) the goethite arms of the star-shaped crystals are shorter, and {021} termination faces of these arms are more abundant (Figs. 4 and 5C–D). It is possible to rationalize both observations by increased phosphate adsorption on the growing faces of the iron oxides at these concentrations. According to Parfitt et al. (1975), and later corroborated by several authors (White 1980; Goldberg and Sposito 1985; Martin and Smart 1987), phosphate can adsorb to goethite through the formation of mono- or binuclear complexes to surface hydroxyls. Recently, we have studied the hydroxyl density on various goethite faces (Barrón and Torrent 1996) and showed that {021} faces have the highest concentration of contiguous singly coordinated hydroxyls. These faces may then preferentially adsorb phosphate and grow slowly, thus keeping the star arms short relative to their width.

ACKNOWLEDGMENTS

This work was supported by the Spanish CICYT in the framework of Project AMB 94-0322. A NATO Research Felowship provided financial support for three months study leave of V.B. at the Virginia Polytechnic Institute. M.F.H. acknowledges the financial assistance of the National Science Foundation through grants EAR-9527092 and EAR-9628023 and also the Petroleum Research Fund (administered by the American Chemical Society) through grant no. 28720-AC2.

REFERENCES CITED

Atkinson, R.J., Posner, A.M., and Quirk, J.P. (1968) Crystal nucleation in Fe(III) solutions and hydroxide gels. Journal of Inorganic and Nuclear Chemistry, 30, 2371–2381.

Barrón, V. and Torrent, J. (1986) Use of the Kubelka-Munk theory to study the influence of iron oxides on soil colour. Journal of Soil Science, 37, 499–510.

——— (1996) Surface hydroxyl configuration of various crystal faces of hematite and goethite. Journal of Colloid and Interface Science, 177, 407–410.

Barton, T.F. (1990) The effect of surface modification on the crystal growth of iron oxides. Ph.D. thesis, 160 p. Virginia Polytechnic Institute and State University, Blacksburg, Virginia.

Blake, R.L., Hessevick, E., Zoltai, T., and Finger, L.W. (1966) Refinement of the hematite structure. American Mineralogist, 51, 123–129.

Blum, A.E. (1994) Determination of illite/smectite particle morphology using scanning force microscopy. In K.L. Nagy and A.E. Blum, Eds., Scanning probe microscopy of clay minerals, p. 172–202. The Clay Minerals Society, Boulder, Colorado.

Bowden, J.W., Nagarajah, S., Barrow, N.J., Posner, A.M., and Quirk, J.Q. (1980) Describing the adsorption of phosphate, citrate and selenite on a variable charge mineral surface. Australian Journal of Soil Research, 18, 49–60.

Cornell, R.M. and Giovanoli, R. (1985) Effect of solution conditions on the proportion and morphology of goethite formed from ferrihydrite. Clays and Clay Minerals, 33, 424–432.

——— (1986) Factors that govern the formation of multi-domainic goethites. Clays and Clay Minerals, 34, 557–564.

Cornell, R.M. and Schwertmann, U. (1996) The iron oxides, 573 p. VCH, New York.

Cornell, R.M., Posner, A.M., and Quirk, J.P. (1974) Crystal morphology and the dissolution of goethite. Journal of Inorganic and Nuclear Chemistry, 36, 1937–1946.

Cornell, R.M., Mann, S., and Skarnulis, A.J. (1983) A high-resolution electron microscopy examination of domain boundaries in crystals of synthetic goethite. Journal of the Chemistry Society. Faraday Transactions I, 79, 2679–2684.

Cornell, R.M., Giovanoli, R., and Schindler, P.W. (1987) Effect of silicate species on the transformation of ferrihydrite into goethite and hematite in alkaline media. Clays and Clay Minerals, 35, 21–28.

Cornell, R.M., Giovanoli, R., and Schneider, W. (1989) Review of the hydrolysis of iron (III) and the crystallization of amorphous iron (III) hydroxide hydrate. Journal of Chemical Technology and Biotechnology, 46, 115–134.

Eggleston, C.M. (1994) High-resolution scanning probe microscopy: tip-surface interaction, artifacts and applications in mineralogy and geochemistry. In K.L. Nagy and A.E. Blum, Eds., Scanning probe microscopy of clay minerals, p. 3–90. The Clay Minerals Society, Boulder, Colorado.

Eggleston, C.M. and Hochella, M.F., Jr. (1992) The structure of hematite (001) surfaces by scanning tunneling microscopy: Image interpretation, surface relaxation, and step structure. American Mineralogist, 77, 911–922.

Eggleston, C.M. and Stumm, W. (1993) Scanning tunneling microscopy of Cr(III) chemisorbed on α-Fe_2O_3(001) surfaces from aqueous solution: Direct observation of surface mobility and clustering. Geochimica et Cosmochimica Acta, 57, 4843–4850.

Fischer, L., Zur Muhlen, E., Brummer, G.W., and Niehus, H. (1996) Atomic force microscopy (AFM) investigations of the surface topography of a multidomain porous goethite. European Journal of Soil Science, 47, 329–334.

Forsyth, J.B., Hedley, I.G., and Johnson, C.E. (1968) The magnetic structure and hyperfine field of goethite (α-FeOOH). Journal of Physical Chemistry, 1, 179–188.

Gibbs, G.V., Boisen, M.B., Downs, R.T., and Bartelmehs, K.L. (1996) X-ray crystallography and powder diffraction methods with computer applications, 187 p. Virginia Tech Press, Blacksburg, Virginia.

Goldberg, S. and Sposito, G. (1985) On the mechanism of phosphate adsorption by hydroxylated mineral surfaces: A review. Communications in Soil Science and Plant Analysis, 16, 801–821.

Junta-Rosso, J.L. and Hochella, M.F., Jr. (1996) The chemistry of hematite (001) surfaces. Geochimica et Cosmochimica Acta, 60, 305–314.

Kandori, K., Uchida, S., Kataoka, S., and Ishikawa, T. (1992) Effects of silicate and phosphate ions on the formation of ferric oxide hydroxide particles. Journal of Materials Science, 27, 719–728.

Lindgreen, H., Garnaes, J., Hansen, P.L., Besenbacher, F., Laegsgaard, I., Gould, S.A.C., and Hansma, P.K. (1991) Ultrafine particles of North Sea illite/smectite clay minerals investigated by STM and AFM. American Mineralogist, 76, 1218–1222.

Martin, R.R. and Smart, R.St.C. (1987) X-ray photoelectron studies of anion adsorption on goethite. Soil Science Society of American Journal, 51, 54–56.

Matijevic, E. (1993) Preparation and properties of uniform size colloids. Chemistry of Materials, 5, 412–426.

Maurice, P.A., Hochella, M.F., Jr., Parks, G.A., Sposito, G., and Schwertmann, U. (1995) Evolution of hematite surface microtopography upon dissolution by simple organic acids. Clays and Clay Minerals, 43, 29–38.

Morales, M.P., González-Carreño, T., and Serna, C.J. (1992) The formation of α-Fe_2O_3 monodispersed particles in solution. Journal of Materials Research, 7, 2539–2444.

Munsell Color Company. (1975) Munsell soil color charts. Munsell Color Co., Baltimore, Maryland.

Nagy, K.L. (1994) Application of morphological data obtained using scanning force microscopy to quantification of fibrous illite growth rates. In K.L. Nagy and A.E. Blum, Eds., Scanning probe microscopy of clay minerals, p. 204–239. The Clay Mineral Society, Boulder, Colorado.

Ocaña, M., Morales, M.P., and Serna, C.J. (1995) The growth mechanism of α-Fe_2O_3 ellipsoidal particles in solution. Journal of Colloid and Interface Science, 171, 85–91.

Parfitt, R.L., Atkinson, R.J., and Smart, R.St.C. (1975) The mechanism of phosphate fixation by iron oxides. Soil Science Society of American Proceedings, 39, 837–841.

Reeves, N.J. and Mann, S. (1991) Influence of inorganic and organic additives on the tailored synthesis of iron oxides. Journal of the Chemical Society, Faraday Transactions, 87, 3875–3880.

Schwertmann, U. (1964) Differenzierung der Eisenoxide des Bodens durch Extraktion mit Ammoniumoxalat-lösung. Zeitschrift für Pflanzenernährung, Düngung und Bodenkunde, 105, 194–202.

——— (1965) Zur Goethitung Hämatitbildung aus amorphem Eisen(III)-hydroxid. Zeitschrift für Pflanzenernährung, Düngung und Bodenkunde, 108, 37–45.

——— (1969) Der Einfluss einfacher organischer Anionen auf die Bildung von Goethit und Hämatit aus amorphem Fe(III)-hydroxid. Geoderma, 3, 207–214.

——— (1984) The influence of aluminum on iron oxides. IX. Dissolution of Al-goethites in 6 M HCl. Clay Minerals, 19, 9–19.

——— (1987). Some properties of soil and synthetic iron oxides. In J. W. Stucky, B.A. Goodman, and U. Schwertmann, Eds., Iron in soils and clay minerals, p. 203–250. NATO Advanced Study Institute, Reidel, Dordrecht.

Schwertmann, U. and Cornell, R.M. (1991) Iron oxides in the laboratory. Preparation and characterization, 236 p. VCH, New York.

Schwertmann, U. and Taylor, R.M. (1989) Iron oxides. In J.B. Dixon and S.B. Weed, Eds., Minerals in soil environments (2nd ed.), p. 379–438. Soil Science Society of America Book Series, Madison, Wisconsin.

Sidhu, P.S., Gilkes, R.J., Cornell, R.M., Posner, A.M., and Quirk, J.P. (1981) Dissolution of iron oxides and oxyhydroxides in hydrochloric and perchloric acids. Clays and Clay Minerals, 29, 269–276.

Sugimoto, T., Muramatsu, A., Sakata, K., and Shindo, D. (1993) Characterization of hematite particles of different shapes. Journal of Colloid and Interface Science, 158, 420–428.

Weidler, P.G., Schwinn, T., and Gaub, H.E. (1996) Vicinal faces on synthetic goethite observed by atomic force microscopy. Clays and Clay Minerals, 44, 437–442.

White, R.E. (1980) Retention and release of phosphate by soils and soil constituents. In P.B. Tinker, Ed., Soils and agriculture, p. 71–114. Halsted Press, New York.

MANUSCRIPT RECEIVED FEBRUARY 5, 1997
MANUSCRIPT ACCEPTED JULY 17, 1997